Computational study of artemisinin interaction with heme and its posterior decomposition

Márcia M. C. Ferreira, Mírian C. S. Perrieira, Rudolf Kiralj. *marcia@iqm.unicamp.br, http://lqta.iqm.unicamp.br*

Laboratório de Quimiometria Teórica e Aplicada (LQTA), Instituto de Química, Universidade Estadual de Campinas, Campinas SP, 13083-970, Brazil

THE OBJECTIVES OF THIS WORK

1) **To determine the global minimum energy conformer of transitional heme-artemisinin complex at the semi-empirical PM3 level, in the presence and absence of water molecules**

2) **To determine thermodinamical, structural and electronic characteristics of reductive artemisinin decomposition, catalyzed by heme iron *via* four main routes: Density Functional Theory (B3LYP 6-31G**), chemometric (exploratory analysis) and structural (Cambridge Structural Database - CSD) are applied**

1 - ARTEMISININ: A NEW POTENT ANTIMALARIAL

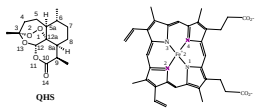

Figure 1. Left: artemisinin (QHS). Right: heme.

Artemisinin (in Chinese: qinghaosu, QHS) is known more than four decades as a natural product from *Artemisia annua*, effective against human antimalaria, including parasites *P. falciparum* and *Plasmodium* strains already resistant against conventional antimalarials. According to the most accepted theory, QHS forms a transitional complex with heme iron, which decomposes into oxygen- or carbon-centered radicals. The radicals follow several decomposition routes in which iron is catalyst. Among species appearing in the decomposition, radicals are species that react with various parasitic molecules. These reactions inhibit parasite denfense and cause its death. Therefore, it is important to have detailed insights into QHS mechanism of action. Such knowledge can be useful in design of more effective antimalarials from the artemisinin class.

2 - CONFORMATIONAL STUDY OF THE HEME-ARTEMISININ COMPLEX

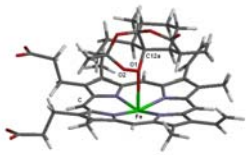

Figure 2. The global minium energy heme-artemisinin complex. Torsion angle C-Fe-O1-C2 is 44° and 52° in absence and presence of water molecules, respectively.

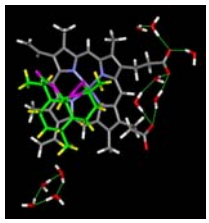

Figure 3. Partially hydrated heme-artemisinin complex. Water-water and water-heme hydrogen bonds are visible.

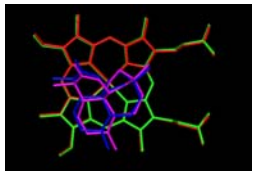

Figure 4. Overlap of hydrated (green/magenta) and free (red/blue) heme-artemisinin complexes. A minor change in conformation is due to partial hydration.

3 - FOUR ARTEMISININ DECOMPOSITION ROUTES

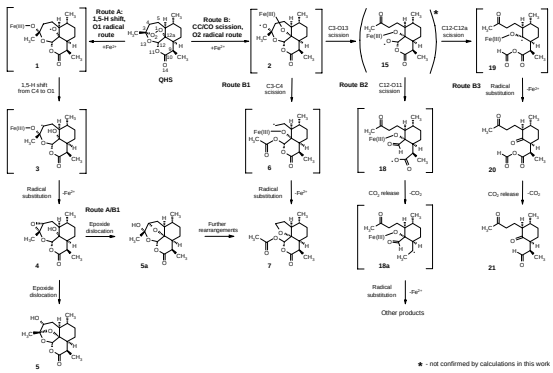

Figure 5. Studied routes A, B1, B2 and B3 of artemisinin decomposition. A/B1 route is a putative connection between A and B1. Radicals are in brackets.

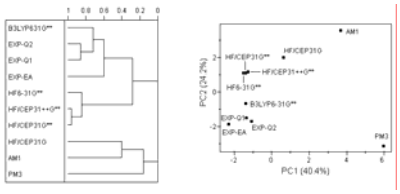

Figure 6. Hierarchial Cluster Analysis (left) and Principal Component Analysis (right) applied to internal coordenates of the 1,2,4-trioxane ring in QHS from various computational methods. B3LYP 6-31G is shown to be the most suitable method for further quantum-chemical calculations. Experimental structures: EXP-Q1, EXP-Q2 and EXP-EA stand for crystal structures with the CSD codes QNGHSU03, QNGHSU10 and WIMMEK, respectively.**

4 - ROUTES A AND B1

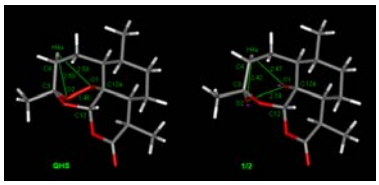

Figure 7. Geometries of QHS and 1/2. Pink ball halves show the radical delocalization between O1 and O2. Interatomic distances before 1,5-hydrogen shift are shown also.

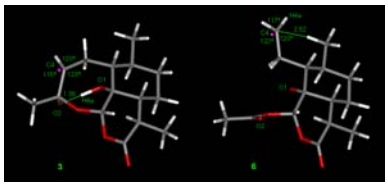

Figure 8. Geometries involving H4α and C4 in 3 and 6. A strong hydrogen bond in 3, a C-H…π interaction in 6 and radical locations are well visible.

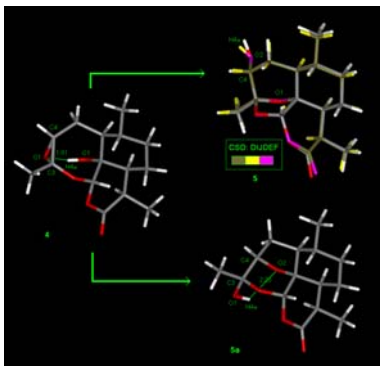

Figure 9. Conversion of intermediate epoxide 4 into 5 and 5a. A strong hydrogen bond in 4 and a weak one in 5a are visible. B3LYP and experimental (CSD: DIJDEF, colored differently) geometries of 5 overlap well.

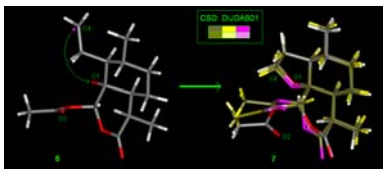

Figure 10. Route B1: Oxidation of radical 6 (pink ball showing the radical localization) into intermediate 7. B3LYP and two experimental (CSD: DIJDAB01, colored differently) geometries of 7 overlap well.

5 - ROUTES B2 AND B3

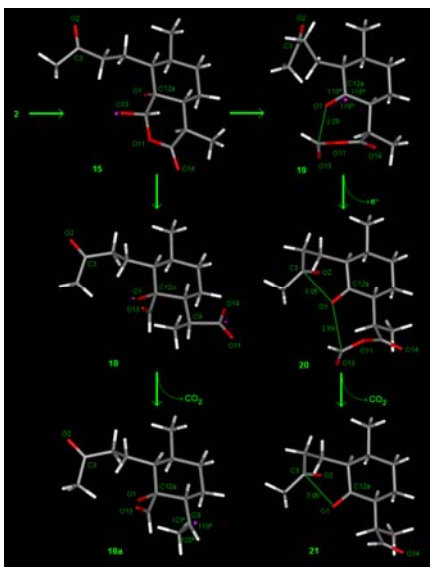

Figure 10. Reaction routes B2 (left) and B3 (right). Interatomic distances involving O1 and bond angles around radicals at C9 and C12a are shown for 18a and 19-21. Pink balls, ball halves and dashed lines show radical localization or partial delocalization.

6 - CHEMOMETRIC COMPARISON OF DECOMPOSITION ROUTES

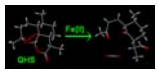

Figure 11. Route B3 (QHS → 21) is thermodinamically the most favorable (ΔΔG = -88 kcal mol^{-1}).

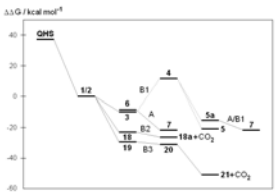

Figure 12. Gibbs free energy diagram for routes of artemisinin decomposition. 4 has uncertain role of in this mechanism.

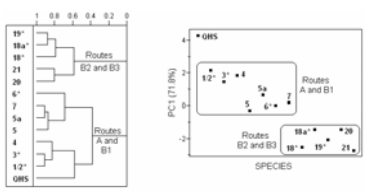

Figure 13. Exploratory analysis of data from Table 1. Left: Hierarchical Cluster Analysis. Right: Principal Component Analysis. Radicals are marked with asterisks (*).

Table 1. Six electronic[a] and structural[b] descriptors of the artemisinin decomposition routes.

Species	E_e/kcal mol^{-1}	ΔG_r/kcal mol^{-1}	d(O1-O2)/Å	<d(O-O)>/Å	lnPLw	<lnPLw>
QHS	33.33	37.25	1.460	3.078	0.1240	-4.3679
1/2	0.00	0.00	2.186	3.211	-1.4619	-4.4146
3	-7.09	-9.73	2.434	3.268	-2.3424	-4.6167
4	8.15	11.55	2.700	3.289	-3.3439	-4.8086
5	-24.29	-20.82	2.806	3.802	-5.1328	-5.1423
5a	-19.65	-15.23	2.713	3.215	-3.9477	-4.6604
7	-22.87	-21.64	2.999	3.133	-5.1850	-4.5148
20	-25.36	-31.15	3.328	4.121	-5.3185	-6.7352
21	-32.61	-51.00	3.328	4.840	-5.3185	-7.8703
6	-0.72	-8.46	4.720	3.518	-5.9915	-4.5479
18	-13.43	-22.97	5.000	5.891	-6.9078	-6.2422
18a	-5.29	-26.32	4.872	4.586	-6.1193	-5.7890
19	-22.40	-29.28	4.812	4.678	-6.5023	-6.0143

[a]**Electronic descriptors: E_e, ΔG_r – electronic energy and free energy relative to 1/2 (including that of CO_2), respectively.**

[b]**Structural descriptors: d(O1-O2) – distance between peroxide oxygen atoms O1 and O2, <d(O-O)> – average oxygen-oxygen distance (CO_2 is excluded), lnPLw – natural logarithm of Löwdin bond order for the O1-O2 distance, and <lnPLw> - average of natural logarithms of Löwdin bond orders for the O-O distances.**

Clustering of the routes into two groups A–B1 and B2 – B3 according to similarity is well noticeable in Figure 13.

7 - CONCLUSIONS

1) **Stereoelectronic interactions define the global minimum energy conformer of heme-artemisinin complex, whilst water does not affect this conformation significantly.**
2) **Among studied routes of reductive artemisinin decomposition, there are two clusters: A–B1 and B2–B3. The former is kinetically and latter is thermodynamically favorable.**
3) **Routes A and B1 are probably interconnected *via* A/B1 route.**
4) **Product 4 probably does not belong to the studied decomposition routes.**
5) **Entropy is the driving force of artemisinin decomposition,**
6) **Along the decomposition routes, following is observed: formation of branched species and CO_2 release, increase of exothermicity, and weakening of attractive O...O interactions.**

ACKNOWLEDGEMENT FAPESP